

Binary Generative Adversarial Networks for Image Retrieval

Jingkuan Song

ABSTRACT

The most striking successes in image retrieval using deep hashing have mostly involved discriminative models, which require labels. In this paper, we use binary generative adversarial networks (BGAN) to embed images to binary codes in an unsupervised way. By restricting the input noise variable of generative adversarial networks (GAN) to be binary and conditioned on the features of each input image, BGAN can simultaneously learn a binary representation per image, and generate an image plausibly similar to the original one. In the proposed framework, we address two main problems: 1) how to directly generate binary codes without relaxation? 2) how to equip the binary representation with the ability of accurate image retrieval? We resolve these problems by proposing new sign-activation strategy and a loss function steering the learning process, which consists of new models for adversarial loss, a content loss, and a neighborhood structure loss. Experimental results on standard datasets (CIFAR-10, NUSWIDE, and Flickr) demonstrate that our BGAN significantly outperforms existing hashing methods by up to 107% in terms of mAP (See Table 3)¹.

KEYWORDS

Generative Adversarial Networks, Hashing, Image Retrieval

ACM Reference format:

Jingkuan Song. 2024. Binary Generative Adversarial Networks for Image Retrieval. In *Proceedings of ACM Conference, Washington, DC, USA, July 2017 (Conference'17)*, 9 pages.
DOI: 10.1145/nnnnnnn.nnnnnnn

1 INTRODUCTION

With the rapidly increasing amount of images, similarity search in large image collections has been actively pursued in a number of domains, including computer vision, information retrieval and pattern recognition [39, 43]. However, exact nearest-neighbor (NN) search is often intractable because of the size of dataset and the high dimensionality of images. Instead, approximate nearest-neighbor (ANN) search is more practical and can achieve orders of magnitude in speed-up compared to exact NN search [18, 39].

Recently, learning-based hashing methods [16, 17, 27, 34, 43, 45] have become the mainstream for scalable image retrieval due to their compact binary representation and efficient Hamming distance

calculation. Such approaches embed data points to compact binary codes through hash functions, which can be generally expressed as:

$$\mathbf{b} = \mathbf{h}(\mathbf{x}) \in \{0, 1\}^L \quad (1)$$

where $\mathbf{x} \in \mathbb{R}^{M \times 1}$, $\mathbf{h}(\cdot)$ are the hash functions, and \mathbf{b} is a binary vector with code length L .

Hashing methods can be generally categorized as being unsupervised or supervised. The unsupervised learning of a hash function is usually based on the criterion of preserving important properties of the training data points in the original space. Typical approaches target pairwise similarity preservation (i.e., the similarity/distance of binary codes should be consistent with that of the original data points) [17, 32, 46], multi-wise similarity preservation (i.e., the similarity orders over more than two items computed from the input space and the coding space should be preserved) [33, 44], or implicit similarity preservation (i.e., pursuing effective space partitioning without explicitly evaluating the relation between the distances/similarities in the input and coding spaces), [15, 19]. A fundamental limitation of a hashing method geared to preserve a particular image property is that its performance may degrade when it is applied to a context where a different property is relevant.

Supervised hashing is designed to generate the binary codes based on predefined labels [8, 27, 40]. For example, Strecha *et al.* [40] developed a supervised hashing which maximizes the between-class Hamming distance and minimizes the within-class Hamming distance. [8, 27] proposed to learn the hash codes such to approximate the pairwise label similarity. Supervised hashing methods usually significantly outperform unsupervised methods. However, the information that can be used for supervision is also typically scarce.

More recently, deep learning has been introduced in the development of hashing algorithms [4, 6, 12, 13, 28, 37, 47], leading to a new generation of *deep hashing* algorithms. Due to powerful feature representation, remarkable image retrieval performance has been reported using the hashes obtained in this way. However, a number of open issues have still remain open. The most successful deep hashing methods are usually supervised and require labels. The labels are, however, scarce and subjective. Unsupervised approaches, on the other hand, cannot take full advantages of the current deep learning models, and thus yield unsatisfactory performance [28]. Another issue is a non-smooth sign-activation function used to generate the binary codes, which, despite several ideas proposed to tackle it [2, 6, 26], still makes the standard back-propagation infeasible.

To address the above issues, we propose an unsupervised hashing method that deploys a generative adversarial network (GAN) [36]. GAN has proven effective to generate synthetic data similar to the training data from a latent space. Therefore, if we restrict the input noise variable of generative adversarial networks (GAN) to be binary and conditioned on the features of each input image, we can learn a binary representation for each image and generate a plausibly similar image to the original one simultaneously. Feeding the generated images through a “discriminator” that verifies them with respect to the training images removes the need for supervision and the

¹Our anonymous code is available at: <https://github.com/htconquer/BGAN>

relevant hash can be learned in an unsupervised fashion. We refer to this proposed architecture as *binary GAN* (BGAN). For the BGAN learning process, we design a novel loss function to equip the binary representation with the ability of accurate image retrieval, beyond vivid image generation. Furthermore, inspired by recent studies on continuation methods [1, 2], we propose two equivalent realizations of the sign-activation function, and design an optimization strategy whose solution is equivalent to the non-smooth sign function.

2 RELATED WORK

2.1 Hashing

Existing hashing methods can be generally divided into two categories: unsupervised, and supervised methods. For unsupervised methods [4, 7, 9, 28, 38], label information is not required in the learning process. For example, Lin *et al.* [28] proposed an unsupervised deep learning approach, DeepBit, imposing three criteria on binary codes (i.e., minimal loss quantization, evenly distributed codes and uncorrelated bits) to learn a compact binary descriptor for efficient visual object matching. The ITQ method proposed by Gong *et al.* [9] maximizes the variance of each binary bit and minimizes the binarization loss to obtain a high performance for image retrieval. Liong *et al.* [7] proposed to use a deep neural network to learn hash codes by optimizing for three objectives: (1) the loss between the real-valued feature descriptor and the learned binary codes is minimized, (2) binary codes distribute evenly on each bit and (3) different bits are as independent as possible.

Supervised hashing methods [6, 12, 13, 26, 37, 47] utilize the label information and can usually obtain better performance. Most of the methods apply pairwise label loss as criterion for optimization. An example is the deep supervised hashing method by Li *et al.* [26], which can simultaneously learn features and hash codes. Another example is Supervised Recurrent Hashing (SRH) for creating video hashes, as proposed by Gu *et al.* [12]. Cao *et al.* [2] proposed a continuous method to learn binary codes, which can avoid the relaxation of binary constraints [12] by first learning continuous representations and then thresholding them to get the hash codes. They also added weight to data for balancing similar and dissimilar pairs.

So far, only supervised hashing methods have been reasonably successful in benefiting from the effectiveness of deep learning. In this paper we address the challenge of enabling an unsupervised method to also take full advantage of this machine learning approach and generate reliable hash codes without the need for class labels.

We also address a specific issue related to the deployment of a deep learning approach in the hashing context, namely that a non-smooth sign-activation function used to generate the binary codes still makes the standard back-propagation infeasible. With our new proposed sign-activation strategy, we provide an effective alternative to earlier attempts to address this issue [2, 6, 26]. For instance, in [2], Cao *et al.* proposed a tanh-like function to replace the sign activation and Li *et al.* introduced an intermediate continuous variable to approximate the binary code [6, 26]. Essentially, they relaxed the binary constraints and the binary codes were further generated by a sign function. Furthermore, the work of Cao *et al.* [2] only considered a special case of solving the non-smooth sign function, instead of looking for a generalized solution.

2.2 Generative Adversarial Nets

Ian *et al.* [11] proposed Generative Adversarial Network (GAN), which has been widely applied in computer vision and natural language processing. In the nutshell, GAN is an architecture for playing a min-max game, where two competing processes aim at maximizing their individual, but mutually conflicting, objectives. GAN has shown its effectiveness in various application contexts and various variants of the original GAN concept have been developed [3, 24, 35]. Radford *et al.* [35] proposed a method for unsupervised feature learning using deep convolutional generative adversarial networks (DCGAN), which was shown to be superior to other unsupervised algorithms. In [24], Larsen *et al.* combined a variational autoencoder (VAE) [21] and GAN to use learned feature representations in the GAN discriminator as the basis for the VAE reconstruction objective. This approach was shown to outperform VAEs with element-wise similarity measures in terms of visual fidelity. In [3], Chen *et al.* proposed a model called Variational InfoGAN (ViGAN), which not only can generate new images based on visual descriptions, but can also retain the latent representation of an image and varying the visual description.

Nevertheless, the learned representations serving as input into the GAN generator in the above methods are not binary. Using a binary image representation in combination with a GAN framework is a new challenge that we address in this paper by proposing *binary generative adversarial networks* (BGAN).

3 BINARY GENERATIVE ADVERSARIAL NETWORKS

Given N images, $\mathbf{I} = \{\mathbf{I}_i\}_{i=1}^N$ without labels, our goal is to learn their compact binary codes \mathbf{B} and reconstructed images \mathbf{I}^R for the original images such that: (a) the binary codes can reconstruct the image content, and (b) the binary codes could be computed directly without relaxation.

We illustrate our proposed BGAN architecture by the scheme in Fig. 1. The scheme shows how hash codes are learned in an unsupervised fashion through the interplay between, on the one side, the image generation process (the generator module) taking the generated hash code (the hash layer) as input, and, on the other side, the verification process (the discriminator module) where the images from the generator are compared to the original training images. For training of the system, we first construct the neighborhood structure of images and then train the neural network underlying the encoder, generator and discriminator. In the remainder of this section, we describe the process of constructing the neighborhood structure, the network architecture, our loss function and learning of parameters.

3.1 Construction of Neighborhood Structure

In our unsupervised approach, we propose to exploit the neighborhood structure of the images in a feature space as information source steering the process of hash learning. Specifically, we propose a method based on the K-Nearest Neighbor (KNN) concept to create a neighborhood matrix \mathbf{S} . Based on [14], we extract 2,048-dimensional features from the pool5-layer. This results in the set $\mathbf{X} = \{\mathbf{x}_i\}_{i=1}^N$ where \mathbf{x}_i is the feature vector of image \mathbf{I}_i .

For the representation of the neighboring structure, our task is to construct a matrix $\mathbf{S} = \{s_{ij}\}_{i,j=1}^N$, whose elements indicate the

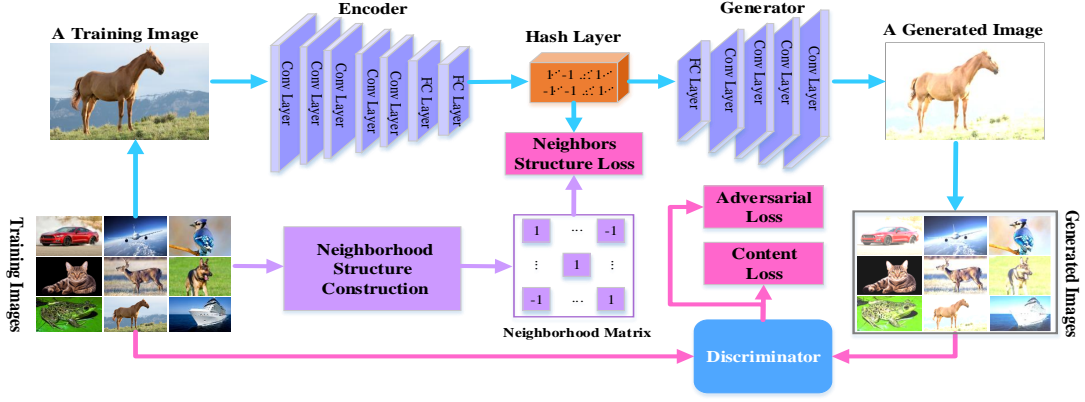


Figure 1: The proposed framework for BGAN, which is comprised of four key components: (1) an encoder, for learning image representations, (2) a hashing layer, for embedding the L-dimensional representation into L-bit binary hash code, (3) a decoder, to reconstruct the original images, and (4) a discriminator, for distinguishing real and reconstructed images. As a pre-processing step, we construct the neighborhood structure of the training images.

similarity ($s_{ij} = 1$) or dissimilarity ($s_{ij} = -1$) of any two images i and j in terms of their features \mathbf{x}_i and \mathbf{x}_j .

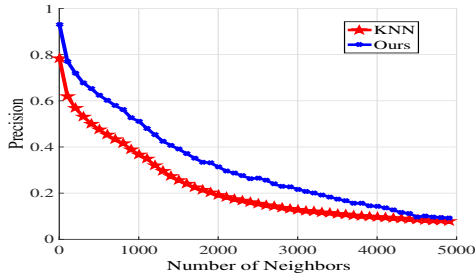


Figure 2: Precision of constructed labels on cifar-10 dataset with different K, and different methods.

We compare images using cosine similarity of the feature vectors. For each image, we select K_1 images with the highest cosine similarity as its neighbors. Then we can construct an initial similarity matrix \mathbf{S}_1 :

$$(\mathbf{S}_1)_{ij} = \begin{cases} 1, & \text{if } \mathbf{x}_j \text{ is } K_1\text{-NN of } \mathbf{x}_i \\ -1, & \text{otherwise} \end{cases} \quad (2)$$

The precision curve (evaluated using the labels) in Figure 2 indicates the quality of the constructed neighborhood for different values of K_1 . Due to rapidly decreasing precision with increasing K_1 , creating a large-enough neighborhood by simply increasing K_1 is not the best option. In order to find a better approach, we borrow the ideas from the domain of graph modeling. In an undirected graph, if a node v is connected to a node u and if u is connected to a node w , we can infer that v is also connected to w . Inspired by this, if we treat every training image as a node in an undirected graph, we can expand the neighborhood of an image i by exploring the neighbors

Algorithm 1 Construct of neighborhood structure

Input: Images $\mathbf{X} = \{\mathbf{x}_i\}_{i=1}^N$, the number of neighbors K_1 , the number of neighbors K_2 for the neighbors expansion;

Output: Neighborhood matrix $\mathbf{S} = \{s_{ij}\}$;

- 1: First ranking: Use cosine similarity to generate the index of K_1 -NN of each image L_1, L_2, \dots, L_N ;
- 2: Neighborhood expansion:
- 3: **for** $j=1, \dots, N$ **do**
- 4: Initialize $num \leftarrow 0$;
- 5: **for** $j=1, \dots, N$ **do**
- 6: $num_j \leftarrow$ the size of $L_i \cap L_j$;
- 7: **end for**
- 8: Sort num by descending order and keep the top $K_2 \{L_j\}$;
- 9: Set new $L'_i \leftarrow$ union of the top $K_2 \{L_j\}$;
- 10: **end for**
- 11: **for** $j=1, \dots, N$ **do**
- 12: Construct \mathbf{S} with new L'_i base on Eq.4;
- 13: **end for**
- 14: **return** \mathbf{S} ;

of its neighbors. Specifically, if \mathbf{x}_i connects to \mathbf{x}_j and \mathbf{x}_j connects to \mathbf{x}_k , we can infer that \mathbf{x}_i has the potential to be also connected to \mathbf{x}_k .

In view of the above, we use the initial similarity matrix \mathbf{S}_1 to expand the neighborhood structure. Specifically, based on \mathbf{S}_1 , we calculate the similarity of two images by comparing the corresponding columns in \mathbf{S}_1 using the expression $\frac{1}{\|(\mathbf{S}_1)_i - (\mathbf{S}_1)_j\|^2}$. Then we again construct a ranked list of K_2 neighbors, based on which we generate the second similarity matrix \mathbf{S}_2 as:

$$(\mathbf{S}_2)_{ij} = \begin{cases} 1, & \text{if } \mathbf{x}_j \text{ is } K_2\text{-NN of } \mathbf{x}_i \\ -1, & \text{otherwise} \end{cases} \quad (3)$$

Finally, we construct the neighborhood structure by combining the direct and indirect similarities from the two matrices together. This

Table 1: The architecture for feature extraction

Layer	Size of Filter	Number of Filters	Others
conv1_1	3x3	64	Stride=1,padding=1,relu
conv1_2	3x3	64	Stride=1,padding=1,relu
Max pooling	2x2		2
conv2_1	3x3	128	Stride=1,padding=1,relu
conv2_2	3x3	128	Stride=1,padding=1,relu
Max pooling	2x2		2
conv3_1	3x3	256	Stride=1,padding=1,relu
conv3_2	3x3	256	Stride=1,padding=1,relu
conv3_3	3x3	256	Stride=1,padding=1,relu
Max pooling	2x2		2
conv4_1	3x3	512	Stride=1,padding=1,relu
conv4_2	3x3	512	Stride=1,padding=1,relu
conv4_3	3x3	512	Stride=1,padding=1,relu
Max pooling	2x2		2
conv5_1	3x3	512	Stride=1,padding=1,relu
conv5_2	3x3	512	Stride=1,padding=1,relu
conv5_3	3x3	512	Stride=1,padding=1,relu
Max pooling	2x2		2
FC6		4096	relu
FC7		4096	relu

results in the final similarity matrix \mathbf{S} :

$$S_{ij} = \begin{cases} 1, & \text{if } (\mathbf{S}_1)_{ij} = 1 \text{ or } \mathbf{x}_j \text{ is a K1-NN of } \mathbf{x}_i \text{ 's K2-NN} \\ -1, & \text{otherwise} \end{cases} \quad (4)$$

The whole algorithm is shown in Alg. 1. We note here that we could have also omitted this preprocessing step and construct the neighborhood structure directly during the learning of our neural network. We found, however, that the construction of neighborhood structure is time-consuming, and that updating of this structure based on the updating of image features in each epoch does not have significant impact on the performance. Therefore, we chose to obtain this neighborhood structure as described above and fix it for the rest of the process.

3.2 Architecture Structure

As shown in Figure 1, our proposed BGAN consists of four components: encoder, hashing, generator and discriminator. We describe each of them in detail in the remainder of this section.

3.2.1 Encoder. For feature extraction, we use a structure similar to VGG19 [41], with the details shown in table 1. We use 5 groups of convolution layers and 5 max convolution-pooling layers. Similar to [41], we use 64, 128, 256, 512, 512 filters in the 5 groups of convolutional layers, respectively.

3.2.2 Hashing. A binary hash code is learned directly, by converting the L -dimensional representation \mathbf{z} learned from the last fully-connected layer FC7, which is continuous in nature, to a binary hash code \mathbf{b} taking values of either +1 or -1. This binarization process can only be performed by taking the sign function $\mathbf{b} = \text{sgn}(\mathbf{z})$ as the activation function on top of the hash layer.

$$\mathbf{b} = \text{sgn}(\mathbf{z}) = \begin{cases} +1, & \text{if } \mathbf{z} \geq 0 \\ -1, & \text{otherwise} \end{cases}$$

Unfortunately, as the sign function is non-smooth and non-convex, its gradient is zero for all nonzero inputs, and is ill-defined at zero, which makes the standard back-propagation infeasible for training deep networks. This is known as the vanishing gradient problem, which has been a key difficulty in training deep neural networks via

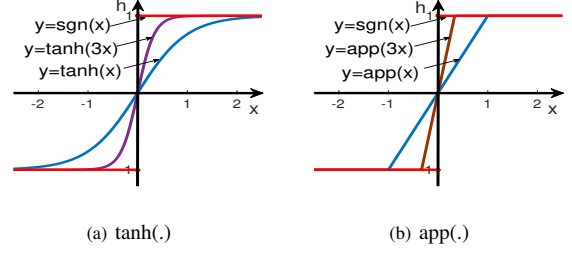


Figure 3: An illustration of the process through which $\text{app}(\cdot)$ approximates $\text{sgn}(\cdot)$

back-propagation [14]. Approximate solutions [20, 48] that relax the binary constraints are not a good alternative as they lead to a large quantization error and therefore to a suboptimal solution [48].

In order to tackle this challenge of optimizing deep networks with non-smooth sign activation, we draw inspiration from recent studies on continuation methods [1, 2]. These studies address a complex optimization problem by smoothing the original function, turning it into a different problem that is easier to optimize. By gradually reducing the amount of smoothing during the training, this results in a sequence of optimization problems converging to the original optimization problem. Following this approach, if we find an approximate smooth function of $\text{sgn}(\cdot)$, and then gradually make the smoothed objective function non-smooth as the training proceeds, the final solution should converge to the desired optimization target.

Motivated by the continuation methods, we define a function $\text{app}(\cdot)$ to approximate $\text{sgn}(\cdot)$:

$$\text{app}(\mathbf{z}) = \begin{cases} +1, & \text{if } \mathbf{z} \geq 1 \\ \mathbf{z}, & \text{if } 1 \geq \mathbf{z} \geq -1 \\ -1, & \text{if } \mathbf{z} \leq -1 \end{cases} \quad (5)$$

We notice that there exists a key relationship between the sign function and the app function in the concept of limit:

$$\text{sgn}(\mathbf{z}) = \lim_{\beta \rightarrow +\infty} \text{app}(\beta \mathbf{z}) \quad (6)$$

An illustration of the process through which $\text{app}(\cdot)$ approximates $\text{sgn}(\cdot)$ is given in Fig. 3. The figure also shows the same process for an alternative to $\text{app}(\cdot)$: $\text{tanh}(\cdot)$:

$$\text{sgn}(\mathbf{z}) = \lim_{\beta \rightarrow +\infty} \tanh(\beta \mathbf{z}) \quad (7)$$

3.2.3 Generator and Discriminator. The task of our BGAN “Generator” network \mathbf{G} is to generate an image based on the hash code \mathbf{b} . First, we let \mathbf{b} serve as the input of the top fully-connected layer with the size $8 \times 8 \times 256$. Then, we use four deconvolutional layers with the size of kernels $5 \times 5, 5 \times 5, 5 \times 5, 1 \times 1$, and the number of kernels 256, 128, 32, 3, which is followed by batch-normalization layers and eLU as the activation function.

Following the approach by Goodfellow et al. [11], we define a “Discriminator” network \mathbf{D} in such a way that it is optimized using criteria that are conflicting to those of \mathbf{G} . In this way, \mathbf{D} can act as adversary to \mathbf{G} in the overall min-max optimization process. The goal of this optimization is to improve \mathbf{G} such to be able to generate the images as well as possible. The process being adversarial to

image generation is the process of trying to distinguish between the original and reconstructed images. If \mathbf{G} manages to generate the images so well to “fool” \mathbf{D} , then it “wins” the min-max game and the overall GAN optimization has converged. In view of this, given a model of the image classifier \mathbf{D} assessing the original (\mathbf{I}) and reconstructed (\mathbf{I}^R) image, we can formally define the min-max game resulting in the optimal system parameters as follows:

$$\min_{\theta_G} \max_{\theta_D} \log(\mathbf{D}(\mathbf{I})) + \log(1 - \mathbf{D}(\mathbf{I}^R)) \quad (8)$$

Here we follow the architecture design summarized by Radford et al. [35], use eLU activation and avoid max-pooling throughout the network. It contains 4 convolutional layers with an increasing number of 5×5 filter kernels (32, 128, 256, and 512). Strided convolutions are used to reduce the image resolution each time the number of features is doubled. The resulting 512 feature maps are followed by a dense layer with the size of 1024 and a final sigmoid activation function to obtain a probability for sample classification.

3.3 Loss Function

The definition of the loss function ℓ is critical for the performance of our network as it steers the overall optimization of the min-max game. While auto-encoding is commonly modeled based on the Mean Squared Error, we follow [24, 25] and design a loss function that assesses our hashing solution with respect to perceptually relevant characteristics. We formulate the loss function as the weighted sum of a neighbor structure loss, content loss and adversarial loss as:

$$\ell = \ell_N + \lambda_1 \ell_C + \lambda_2 \ell_A \quad (9)$$

In the following subsections, we explain our realization of each of the loss functions.

3.3.1 Neighbors Structure Loss. The neighborhood structure loss models the loss in the similarity structure in data, as revealed in the set of neighbors obtained for an image by applying the hash code of that image. Given the binary codes $\mathbf{B} = \{\mathbf{b}_i\}_{i=1}^N$ for all the images of the length L , and using the similarity matrix \mathbf{S} as the reference for similarity relations between images, we define the neighbors structure loss as follows:

$$\ell_N = \frac{1}{2} \sum_{s_{ij} \in \mathbf{S}} \left(\frac{1}{L} \mathbf{b}_i^T \mathbf{b}_j - s_{ij} \right)^2 \quad (10)$$

The goal of optimizing for this loss function is clearly to bring the binary codes of similar images as close to each other as possible.

3.3.2 Content Loss. The content loss models the loss in the quality of reconstructed images. The most widely used pixel-wise MSE loss is calculated as:

$$\ell_{MSE} = \frac{1}{WH} \sum_{i=1}^W \sum_{j=1}^H (I_{ij} - I_{ij}^R)^2 \quad (11)$$

However, as pointed out in [25], solutions of MSE optimization problems often lack high-frequency content, which results in perceptually unsatisfying solutions with overly smooth textures. Also, element-wise reconstruction errors are not robust for images and other signals with invariance.

Therefore, instead of only relying on pixel-wise losses we build on the ideas of Christian et. al. [25] and use a loss function that closer

resembles perceptual similarity. Specifically, we define the VGG loss based on the eLU activation layers of the last convolutional layer of our discriminator networks \mathbf{D} . With ϕ we indicate the feature map obtained by the last convolution (after activation) and then define the VGG loss as the Euclidean distance between the feature representations of a reconstructed image I^R and the original image I :

$$\ell_{Perceptual} = \frac{1}{WH} \sum_{i=1}^W \sum_{j=1}^H \left(\phi(I_{ij}) - \phi(I_{ij}^R) \right)^2 \quad (12)$$

Here, W and H represent the dimensions of the respective feature maps. Based on the above, we can now define the content loss as:

$$\ell_C = \ell_{MSE} + \ell_{Perceptual}. \quad (13)$$

3.3.3 Adversarial Loss: The adversarial loss models the loss due to misclassification of images, as done by \mathbf{D} , in the original and reconstructed ones. Using the notations already explained in the context of Eq.8, we model this loss as:

$$\ell_A = \log(\mathbf{D}(\mathbf{I})) + \log(1 - \mathbf{D}(\mathbf{I}^R)) \quad (14)$$

3.4 Learning

Using the loss function in Eq.9, we train our network. The forward propagation is as follows. First, we use a deep convolutional network as the encoder to extract the features and then use hash layer to obtain to embed the real-valued features into binary codes:

$$\mathbf{b}_i = \text{sgn}(\mathbf{W}_h^T \varphi(\mathbf{I}_i; \theta)) \quad (15)$$

where \mathbf{I}_i is an input image, θ is the parameter of the encoder and \mathbf{W}_h stands for the parameter of generating \mathbf{Z} . Then, \mathbf{b}_i is the input for a generator \mathbf{G} to reconstruct an image \mathbf{I}^R :

$$\mathbf{I}_i^R = \phi(\mathbf{b}_i; \pi) \quad (16)$$

where π stands for the parameters of the generator \mathbf{G} . Finally, a discriminator \mathbf{D} assigns probability:

$$p = \mathbf{D}(\mathbf{I}_i^R; \psi) \quad (17)$$

that \mathbf{I}_i^R is an actual training sample and probability $1 - p$ that \mathbf{I}_i^R is generated by our model $\mathbf{I}_i^R = \phi(\mathbf{b}_i; \pi)$.

In the network, we have parameters of θ , π , ψ and \mathbf{W}_h to learn. We use back-propagation (BP) for learning and stochastic gradient descent (SGD) to minimize the loss. In particular, we initialize network parameters and use forward propagation to obtain the value of each loss (ℓ_N, ℓ_C, ℓ_A). In each iteration, we sample a mini-batch of images from the training set, and then update each parameter:

$$\theta \leftarrow \theta - \tau \nabla_{\theta} (\ell_N + \ell_C), \quad (18)$$

$$\pi \leftarrow \pi - \tau \nabla_{\pi} (\ell_C + \ell_A), \quad (19)$$

$$\psi \leftarrow \psi + \tau \nabla_{\psi} \ell_A, \quad (20)$$

$$\mathbf{W}_h \leftarrow \mathbf{W}_h - \tau \nabla_{\mathbf{W}_h} (\ell_N + \ell_C) \quad (21)$$

where τ is the learning rate. We train our network until it converges.

For the hashing layer, we start training BGAN with $\beta_t = 1$. For each stage t , after BGAN converges, we increase β_t and train (i.e., fine-tune) BGAN by setting the converged network parameters as the initialization for training the BGAN in the next stage. By evolving $\text{app}(\beta \mathbf{z})$ with $\beta_t \approx \infty$, the network will converge to BGAN with $\text{sgn}(\mathbf{z})$ as activation function, which can generate exactly binary hash

codes as we desire. Using $\beta_t = 10$ we can already achieve fast convergence for training BGAN.

4 EXPERIMENTS

We evaluate our BGAN on the task of large-scale image retrieval. Specifically, the experiments are designed to study the following research questions of our algorithm:

RQ1: How does each component of our algorithm affect the performance?

RQ2: Does the binary codes computed directly without relaxation improve the performance of the relaxed resolution?

RQ3: Does the performance of BGAN significantly outperform the state-of-the-art hashing algorithms?

RQ4: What is the efficiency of BGAN?

4.1 Settings

4.1.1 Datasets. We conduct empirical evaluation on three public benchmark datasets, CIFAR-10, NUS-WIDE, and Flickr.

CIFAR-10 labeled subsets of the 80 million tiny images dataset, which consists of 60,000 32×32 color images in 10 classes, with 6,000 images per class.

NUS-WIDE is a web image dataset containing 269,648 images downloaded from Flickr. Tagging ground-truth for 81 semantic concepts is provided for evaluation. We follow the settings in [49] and use the subset of 195,834 images from the 21 most frequent concepts, where each concept consists of at least 5,000 images.

Flickr is a collection of 25,000 images from Flickr, where each image is labeled with one of the 38 concepts. We resize images of this subset into 256×256 .

In NUS-WIDE and CIFAR-10, we randomly select 100 images per class as the test query set, and 1,000 images per class as the training set. In Flickr, we randomly select 1,000 images as the test query set, and 4,000 images as the training set.

4.1.2 Evaluation Metric. Hamming ranking is used as the search protocol to evaluate our proposed approaches, and two indicators are reported. 1) **Mean Average Precision (mAP):** For a single query, Average Precision (AP) is the average of the precision value obtained for the set of top-k results, and this value is then averaged over all the queries. 2) **Precision:** We further use precision-recall curve and precision@K to evaluate the precision of retrieved images at each stage.

4.1.3 Compared algorithms. We compare our BGAN with other state-of-the-art hashing algorithms. Specifically, we compare with four non-deep hashing methods (iterative quantization (ITQ) hashing [10], spectral hashing (SH) [46], Locality Sensitive Hashing (LSH) [5] and spherical hashing [15]), and two deep hashing methods (DeepBit [28] and Deep Hashing (DH) [7]).

To make a fair comparison, we also apply the non-deep hashing methods on deep features extracted by the CNN-F of the feature learning part in our BGAN. For non-deep hashing algorithms, we use 1134-D concatenated features as the hand-crafted features, including 64-D color histogram, 144-D color correlogram, 73-D edge direction histogram, 128-D wavelet texture, 225-D block-wise color moments and 500-D bag of words based on SIFT descriptions.

We also conduct the non-deep hashing methods on deep features extracted by the VGG network (VGG-fc7 [41]). For non-deep hashing algorithms, we use 512-dim GIST features as the hand-crafted features. We also compare with PCAH [42], DGH [29], AGH [31], and UN-BDNH [6] in term of precision.

By constructing the neighborhood structure using the labels, our method can be easily modified as a supervised hashing method. Therefore, we also compare with some supervised hashing methods, e.g., iterative quantization hashing (ITQ-CCA) [10], KSH [30], minimal loss hashing (MLH) [33], DNNH [23], CNNH [37] and Deep Hashing Network (DHN) [49].

4.1.4 Implementation Details. In the construction of neighborhood structure step, we set $K_1 = 20$, $K_2 = 30$ for CIFAR-10 dataset, and the average number of the neighbors for each image is 400, 1021, 1168 for the three datasets. By default, we set $\lambda_1 = 0.1$ and $\lambda_2 = 0.1$. We set the mini-batch size as 256, and the learning rate as 0.01.

4.2 Component Analysis (RQ1)

Our loss function consists of three major components: neighborhood structure loss (ℓ_N), content loss (ℓ_C) and adversarial loss (ℓ_A). In this subsection, we study the effect of each component on the performance. Due to the space limit, we only report the results on the CIFAR-10 dataset in Table 2. An interesting observation is that if we do not use the neighborhood structure loss (ℓ_N), we will learn identical hash codes for all the images. A possible reason is that when we define no loss function directly on the hash codes, the loss from ℓ_C and ℓ_A in the back-propagation step cannot well guide the learning of hashing codes. Another interesting finding is that using the combination of ℓ_N and ℓ_C , or the combination of ℓ_N and ℓ_A can obtain even worse performance than using ℓ_N only. The is understandable, because if we use ℓ_N and ℓ_C without ℓ_A , the discriminator network **D** based on ℓ_A cannot learn satisfactory features. Thus, the loss function ℓ_C based on the features of **D** will mislead the learning of hash codes. It is the same case for the unsatisfactory performance of ℓ_N and ℓ_A . When we only force the reconstructed images to be similar to the general images, without considering its similarity to the corresponding input images, the performance of the learned hash codes will also be degraded.

The best performance is achieved when we use the combination of the three components: $\ell_N + \ell_C + \ell_A$. Compared with using ℓ_N only, the performance is improved by 2.5%, 2% and 1.3% for 24, 32,

Table 2: The mAP of BGAN on CIFAR-10 using different combinations of components.

Components	mAP		
	24-bit	32-bit	48-bit
ℓ_N	0.487	0.511	0.543
ℓ_C	-	-	-
ℓ_A	-	-	-
$\ell_N + \ell_C$	0.247	0.379	0.497
$\ell_N + \ell_A$	0.472	0.503	0.534
$\ell_C + \ell_A$	-	-	-
$\ell_N + \ell_C + \ell_A$	0.512	0.531	0.558

Table 3: mAP for different unsupervised hashing methods using different number of bits on three image datasets

Method	CIFAR-10				NUS-WIDE				Flickr			
	12 bits	24 bits	32 bits	48 bits	12 bits	24 bits	32 bits	48 bits	12 bits	24 bits	32 bits	48 bits
ITQ [10]	0.162	0.169	0.172	0.175	0.452	0.468	0.472	0.477	0.544	0.555	0.560	0.570
SH [46]	0.131	0.135	0.133	0.130	0.433	0.426	0.426	0.423	0.531	0.533	0.531	0.529
LSH [5]	0.121	0.126	0.120	0.120	0.403	0.421	0.426	0.441	0.499	0.513	0.521	0.548
Spherical [15])	0.138	0.141	0.146	0.150	0.413	0.413	0.424	0.431	0.569	0.559	0.583	0.572
ITQ+VGG	0.196	0.246	0.289	0.301	0.435	0.435	0.548	0.435	0.553	0.548	0.545	0.560
SH+VGG	0.174	0.205	0.220	0.232	0.433	0.426	0.426	0.423	0.550	0.544	0.541	0.545
LSH+VGG	0.101	0.128	0.132	0.169	0.401	0.442	0.480	0.471	0.543	0.549	0.555	0.551
Spherical+VGG	0.212	0.247	0.256	0.281	0.549	0.614	0.653	0.678	0.552	0.547	0.546	0.545
DeepBit [28]	0.185	0.218	0.248	0.263	0.383	0.401	0.403	0.412	0.501	0.505	0.511	0.513
DH [7]	0.160	0.164	0.166	0.168	0.422	0.448	0.480	0.493	0.553	0.548	0.543	0.556
BGAN	0.401	0.512	0.531	0.558	0.675	0.690	0.714	0.728	0.683	0.702	0.703	0.703

and 48-bit hash codes, which is not that significant. From the above analysis, we can conclude that all these three components contribute to the great performance of our BGAN.

4.3 Effect of Binary Optimization (RQ2)

As discussed above, BGAN can learn binary hash codes directly while previous hashing methods first learn continuous representations and then generate hash codes using a sign function as post-process. In this subsection, we study the effect of direct binary codes optimization on the performance of hash codes, and the results are shown in Table 4. As shown in Table 4, our binary optimization can improve the performance of the learned binary codes. Specifically, the first solution (Eq.6) outperforms two-step solution by 2.5%, 3.2%, and 2.3% for 24, 32, and 48-bit hash codes. While the second solution (Eq.7) improves it by 3.0%, 4.6%, and 2.8%. This verifies our argument that two-step solution is sub-optimal, and binary optimization can achieve a better performance.

Table 4: The mAP of BGAN on CIFAR-10 using different combinations of components.

Methods	mAP		
	24-bit	32-bit	48-bit
two-step solution	0.512	0.531	0.558
$\text{sgn}(z) = \lim_{\beta \rightarrow +\infty} \tanh(\beta z)$	0.542	0.577	0.586
$\text{sgn}(z) = \lim_{\beta \rightarrow +\infty} \text{app}(\beta z)$	0.537	0.563	0.581

4.4 Compare with the State-of-the-art Algorithms (RQ3)

In this subsection, we compare our BGAN with different unsupervised hashing methods on three datasets. The results on mAP are shown in Table 3, and the precision is shown in Fig. 4. From Table 3 and Fig. 4, we have the following observations:

1) Our method significantly outperforms the other deep or non-deep hashing methods in all datasets. In CIFAR-10, the improvement of BGAN over the other methods is more significant, compared with that in NUS-WIDE and Flickr datasets. Specifically, it outperforms the best counterpart (Spherical+VGG) by 18.9%, 26.5%, 27.5%

Table 5: mAP for different supervised hashing methods using different number of bits on three image datasets

Method	CIFAR-10			
	12 bits	24 bits	32 bits	48 bits
ITQ-CCA [10]	0.435	0.435	0.435	0.435
KSH [30]	0.556	0.572	0.581	0.588
MLH [33]	0.500	0.514	0.520	0.522
DNNH [23]	0.674	0.697	0.713	0.715
CNNH[37]	0.611	0.618	0.625	0.608
DHN [49]	0.708	0.735	0.748	0.758
BGAN	0.866	0.874	0.876	0.877

and 27.7% for 12, 24, 32 and 48-bit hash codes. One possible reason is that CIFAR-10 contains simple images, and the constructed neighborhood structure is more accurate than the other two datasets. BGAN improves the state-of-the-arts by 12.6%, 7.6%, 6.1% and 5.0% in NUS-WIDE dataset, and 11.4%, 14.3%, 12.0% and 13.1% in NUS-WIDE dataset.

2) Table 3 shows that Spherical+VGG is a strong competitor in terms of mAP, and Fig. 4 performs well for small number of retrieved samples (or recall). On the other hand, the performance of deep hashing methods (DeepBit [28] and DH [7]) is not superior. A possible reason is the deep hashing methods use only 3 full connected layers to extract the features, which is not very powerful.

3) When we run the non-deep hashing methods on deep features, the performance is usually improved compared with the hand-crafted features. The performance gap is larger in CIFAR-10 and NUS-WIDE datasets than in Flickr dataset.

4) With the increase of code length, the performance of most hashing methods is improved accordingly. More specifically, the mAP improvements using deep features are generally more significant than that of non-deep features in CIFAR-10 dataset and NUS-WIDE dataset. An exception is SH, which has no improvement with the increase of code length.

We also compared with supervised hashing methods, and shown the mAP results on CIFAR-10 dataset in Table 6. It is obvious that our BGAN_s outperforms the state-of-the-art deep and non-deep supervised hashing algorithms by a large margin, which are 15.8%, 13.9%, 12.8% and 11.9% for 12, 24, 32, and 48-bits hash codes. This

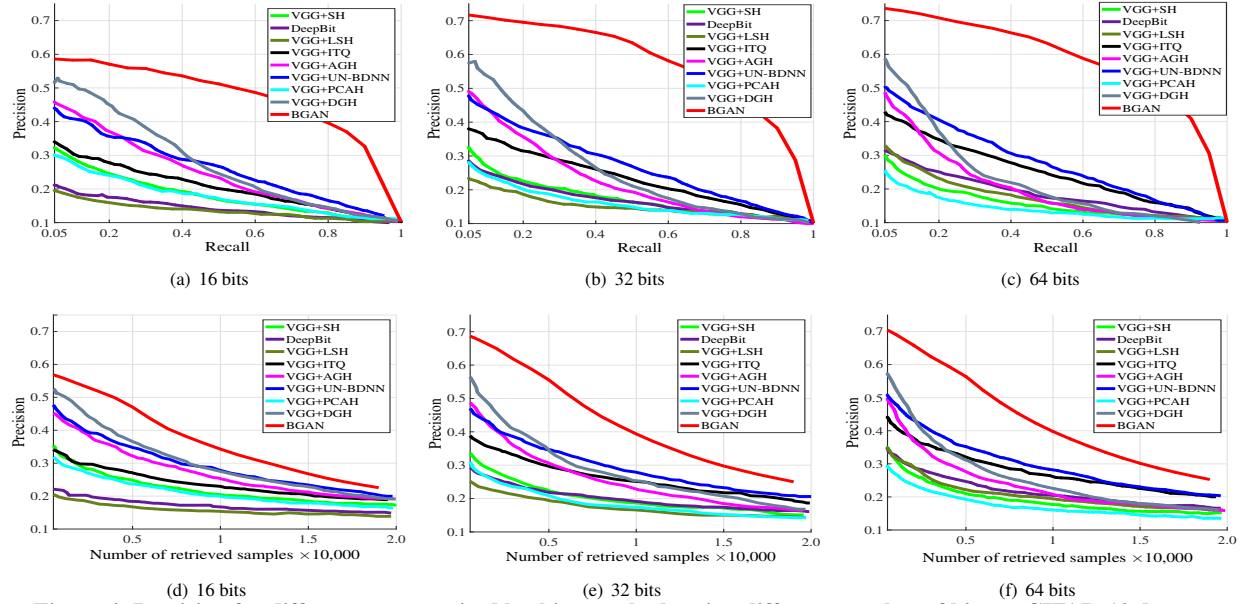


Figure 4: Precision for different unsupervised hashing methods using different number of bits on CIFAR-10 dataset.

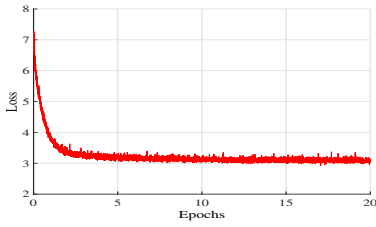


Figure 5: The convergence of BGAN in CIFAR-10 dataset.

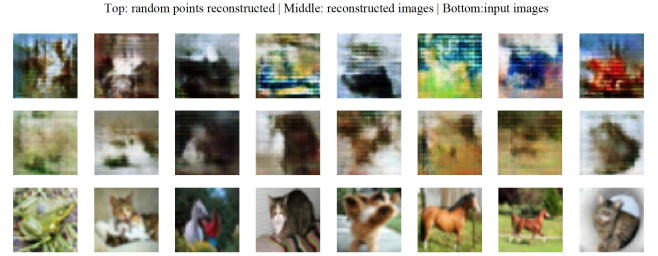


Figure 6: Image reconstruction using binary codes.

indicates that the performance improvement of BGAN is not only due to the constructed neighborhood structure, but also the other components.

4.5 The Study of Efficiency (RQ4)

In this subsection, we study the efficiency of our algorithm. First, we study the convergence of our BGAN in CIFAR-10 dataset, and the results are shown in Fig. 5. It can be seen that our method converges after a few epochs, which shows the efficiency of our solution.

We also report the training and testing time in CIFAR-10 dataset of our algorithm, and compare it with DH [7] in Table 6. Since our BGAN has more parameters, it takes longer time for training and testing. However, BGAN is still very fast for generating the hash codes for a test image.

Table 6: The training and testing time for BGAN and DH.

Methods	Training time	Testing time
DH [7]	1 hour	0.5 ms
BGAN	5h	3 ms

4.6 Reconstruction Results

To evaluate the ability of image reconstruction using BGAN, we show some qualitative results on CIFAR-10 dataset in Fig. 6. The top row are the reconstructed results using random input, the second row are the reconstructed results from BGAN, and the last row are the original images. We can see that BGAN can reconstruct images which are similar to the original images.

5 CONCLUSION

In this work, we propose an unsupervised hashing which addresses two central problems remaining largely unsolved for image hashing: 1) how to directly generate binary codes without relaxation? 2) how to equip the binary representation with the ability of accurate image retrieval, beyond vivid image generation? First, we propose two equivalent but smoothed activation functions, and design a learning strategy whose solution converges to the results of sign activation. Second, we propose a loss function which consists of an adversarial loss, a content loss, and a neighborhood structure loss. Experimental results show that our BGAN doubled the performance of the state-of-the-arts in CIFAR-10 dataset, and also significantly outperformed

the others on NUSWIDE, and Flickr datasets. In the future, it is necessary to improve the reconstruction accuracy of BGAN.

REFERENCES

- [1] Eugene L. Allgower and Kurt Georg. 2012. *Numerical continuation methods: an introduction*. Vol. 13. Springer Science & Business Media.
- [2] Zhangjie Cao, Mingsheng Long, Jianmin Wang, and Philip S Yu. 2017. HashNet: Deep Learning to Hash by Continuation. *arXiv preprint arXiv:1702.00758* (2017).
- [3] Xi Chen, Yan Duan, Rein Houthoofd, John Schulman, Ilya Sutskever, and Pieter Abbeel. 2016. InfoGAN: Interpretable Representation Learning by Information Maximizing Generative Adversarial Nets. (2016).
- [4] Qi Dai, Jinguo Li, Jingdong Wang, and Yu-Gang Jiang. 2016. Binary Optimized Hashing. In *ACM Multimedia*. ACM, 1247–1256.
- [5] Mayur Datar, Nicole Immorlica, Piotr Indyk, and Vahab S. Mirrokni. 2004. Locality-sensitive hashing scheme based on p-stable distributions. In *Symposium on Computational Geometry*.
- [6] Thanh-Toan Do, Anh-Dzung Doan, and Ngai-Man Cheung. 2016. Learning to hash with binary deep neural network. In *ECCV*. Springer, 219–234.
- [7] Venice Erin Liong, Jiwen Lu, Gang Wang, Pierre Moulin, and Jie Zhou. 2015. Deep hashing for compact binary codes learning. In *Proceedings of the IEEE Conference on Computer Vision and Pattern Recognition*. 2475–2483.
- [8] Tiezheng Ge, Kaiming He, and Jian Sun. 2014. Graph Cuts for Supervised Binary Coding. In *ECCV*.
- [9] Y. Gong, S Lazebnik, A Gordo, and F Perronnin. 2013. Iterative quantization: a Procrustean approach to learning binary codes for large-scale image retrieval.. In *IEEE Conference on Computer Vision and Pattern Recognition*. 817–824.
- [10] Yunchao Gong, Svetlana Lazebnik, Albert Gordo, and Florent Perronnin. 2013. Iterative Quantization: A Procrustean Approach to Learning Binary Codes for Large-Scale Image Retrieval. *IEEE Trans. PAMI* 35, 12 (2013), 2916–2929.
- [11] Ian Goodfellow, Jean Pouget-Abadie, Mehdi Mirza, Bing Xu, David Warde-Farley, Sherjil Ozair, Aaron Courville, and Yoshua Bengio. 2014. Generative adversarial nets. In *Advances in neural information processing systems*. 2672–2680.
- [12] Yun Gu, Chao Ma, and Jie Yang. 2016. Supervised Recurrent Hashing for Large Scale Video Retrieval. In *Proceedings of the 2016 ACM on Multimedia Conference*. ACM, 272–276.
- [13] Jinma Guo, Shifeng Zhang, and Jianmin Li. 2016. Hash learning with convolutional neural networks for semantic based image retrieval. In *Pacific-Asia Conference on Knowledge Discovery and Data Mining*. Springer, 227–238.
- [14] Kaiming He, Xiangyu Zhang, Shaoqing Ren, and Jian Sun. 2015. Deep Residual Learning for Image Recognition. *arXiv preprint arXiv:1512.03385* (2015).
- [15] Jae-Pil Heo, Youngwoon Lee, Junfeng He, Shih-Fu Chang, and Sung-Eui Yoon. 2015. Spherical Hashing: Binary Code Embedding with Hyperspheres. *IEEE Trans. Pattern Anal. Mach. Intell.* 37, 11 (2015), 2304–2316.
- [16] Yao Hu, Zhongming Jin, Hongyi Ren, Deng Cai, and Xiaofei He. 2014. Iterative Multi-View Hashing for Cross Media Indexing. In *ACM MM*.
- [17] Go Irie, Zhenguo Li, Xiao-Ming Wu, and Shih-Fu Chang. 2014. Locally Linear Hashing for Extracting Non-linear Manifolds. In *CVPR*.
- [18] Hervé Jégou, Matthijs Douze, and Cordelia Schmid. 2011. Product Quantization for Nearest Neighbor Search. *IEEE Trans. PAMI* 33, 1 (2011), 117–128.
- [19] Zhongming Jin, Yao Hu, Yue Lin, Debing Zhang, Shiding Lin, Deng Cai, and Xuelong Li. 2013. Complementary Projection Hashing. In *IEEE International Conference on Computer Vision, ICCV 2013, Sydney, Australia, December 1-8, 2013*. 257–264.
- [20] Wang-Cheng Kang, Wu-Jun Li, and Zhi-Hua Zhou. 2016. Column Sampling based Discrete Supervised Hashing. In *AAAI*.
- [21] Diederik P Kingma and Max Welling. 2013. Auto-encoding variational bayes. *arXiv preprint arXiv:1312.6114* (2013).
- [22] Alex Krizhevsky, Ilya Sutskever, and Geoffrey E Hinton. 2012. Imagenet classification with deep convolutional neural networks. In *Advances in neural information processing systems*. 1097–1105.
- [23] Hanjiang Lai, Yan Pan, Ye Liu, and Shuicheng Yan. 2015. Simultaneous feature learning and hash coding with deep neural networks. In *CVPR*. 3270–3278.
- [24] Anders Boesen Lindbo Larsen, Søren Kaae Sønderby, Hugo Larochelle, and Ole Winther. 2015. Autoencoding beyond pixels using a learned similarity metric. *arXiv preprint arXiv:1512.09300* (2015).
- [25] Christian Ledig, Lucas Theis, Ferenc Huszar, Jose Caballero, Andrew P. Aitken, Alykhan Tejani, Johannes Totz, Zehan Wang, and Wenzhe Shi. 2016. Photo-Realistic Single Image Super-Resolution Using a Generative Adversarial Network. *CoRR abs/1609.04802* (2016).
- [26] Wu Jun Li, Sheng Wang, and Wang Cheng Kang. 2015. Feature Learning based Deep Supervised Hashing with Pairwise Labels. *Computer Science* (2015).
- [27] Guosheng Lin, Chunhua Shen, Qinfeng Shi, Anton van den Hengel, and David Suter. 2014. Fast Supervised Hashing with Decision Trees for High-Dimensional Data. In *CVPR*.
- [28] Kevin Lin, Jiwen Lu, Chu-Song Chen, and Jie Zhou. 2016. Learning compact binary descriptors with unsupervised deep neural networks. In *Proceedings of the IEEE Conference on Computer Vision and Pattern Recognition*. 1183–1192.
- [29] Wei Liu, Cun Mu, Sanjiv Kumar, and Shih-Fu Chang. 2014. Discrete Graph Hashing. In *NIPS*. 3419–3427.
- [30] Wei Liu, Jun Wang, Rongrong Ji, Yu-Gang Jiang, and Shih-Fu Chang. 2012. Supervised hashing with kernels. In *CVPR*.
- [31] Wei Liu, Jun Wang, Sanjiv Kumar, and Shih-Fu Chang. 2011. Hashing with Graphs. In *ICML*.
- [32] Xianglong Liu, Junfeng He, Cheng Deng, and Bo Lang. 2014. Collaborative Hashing. In *CVPR*.
- [33] Mohammad Norouzi and David J. Fleet. 2011. Minimal Loss Hashing for Compact Binary Codes. In *ICML*.
- [34] Mohammad Norouzi and David J. Fleet. 2013. Cartesian K-Means. In *CVPR*.
- [35] Alec Radford, Luke Metz, and Soumith Chintala. 2015. Unsupervised representation learning with deep convolutional generative adversarial networks. *arXiv preprint arXiv:1511.06434* (2015).
- [36] Scott Reed, Zeynep Akata, Xincheng Yan, Lajanugen Logeswaran, Bernt Schiele, and Honglak Lee. 2016. Generative Adversarial Text to Image Synthesis. (2016).
- [37] Hanjiang Lai Cong Liu Rongkai Xia, Yan Pan and Shuicheng Yan. 2014. Supervised Hashing for Image Retrieval via Image Representation Learning. In *AAAI*. 2156–2162.
- [38] Ruslan Salakhutdinov and Geoffrey Hinton. 2009. Semantic hashing. *International Journal of Approximate Reasoning* 50, 7 (2009), 969–978.
- [39] Gregory Shakhnarovich, Trevor Darrell, and Piotr Indyk. 2008. Nearest-Neighbor Methods in Learning and Vision. *IEEE Transactions on Neural Networks* 19, 2 (2008), 377.
- [40] Christoph Strecha, Alexander M Bronstein, Michael M Bronstein, and Pascal Fua. 2012. LDAHash: Improved matching with smaller descriptors. *IEEE Trans. Pattern Anal. Mach. Intell.* 34, 1 (2012), 66–78.
- [41] Christian Szegedy, Wei Liu, Yangqing Jia, Pierre Sermanet, Scott Reed, Dragomir Anguelov, Dumitru Erhan, Vincent Vanhoucke, and Andrew Rabinovich. 2015. Going deeper with convolutions. In *Proceedings of the IEEE Conference on Computer Vision and Pattern Recognition*. 1–9.
- [42] Jun Wang, Sanjiv Kumar, and Shih-Fu Chang. 2012. Semi-Supervised Hashing for Large-Scale Search. *IEEE Trans. PAMI* 34, 12 (2012), 2393–2406.
- [43] Jingdong Wang, Heng Tao Shen, Jingkuan Song, and Jianqiu Ji. 2014. Hashing for Similarity Search: A Survey. *CoRR abs/1408.2927* (2014).
- [44] Jianfeng Wang, Jingdong Wang, Nenghai Yu, and Shipeng Li. 2013. Order preserving hashing for approximate nearest neighbor search. In *ACM MM*.
- [45] Qifan Wang, Luo Si, and Dan Zhang. 2014. Learning to Hash with Partial Tags: Exploring Correlation between Tags and Hashing Bits for Large Scale Image Retrieval. In *ECCV*.
- [46] Yair Weiss, Antonio Torralba, and Robert Fergus. 2008. Spectral Hashing. In *NIPS*.
- [47] Hui-Fang Yang, Kevin Lin, and Chu-Song Chen. 2017. Supervised Learning of Semantics-Preserving Hash via Deep Convolutional Neural Networks. *IEEE Transactions on Pattern Analysis and Machine Intelligence* (2017).
- [48] Peichao Zhang, Wei Zhang, Wu-Jun Li, and Minyi Guo. 2014. Supervised Hashing with Latent Factor Models. In *Proceedings of the 37th International ACM SIGIR Conference on Research & Development in Information Retrieval (SIGIR '14)*. 173–182.
- [49] Han Zhu, Mingsheng Long, Jianmin Wang, and Yue Cao. 2016. Deep Hashing Network for Efficient Similarity Retrieval.. In *AAAI*. 2415–2421.